Inorganic Chemistry

Article

pubs.acs.org/IC

Reaction of Laser-Ablated Uranium and Thorium Atoms with H_2Se: A Rare Example of Selenium Multiple Bonding

Thomas Vent-Schmidt,[†] Lester Andrews,*[,‡] K. Sahan Thanthiriwatte,[§] David A. Dixon,*[,§] and Sebastian Riedel*[,∥]

[†]Institut für Anorganische und Analytische Chemie, Albert-Ludwigs-Universität Freiburg, Albertstraße 21, D-79104 Freiburg i. Br., Germany

[‡]Department of Chemistry, University of Virginia, P.O. Box 400319, Charlottesville, Virginia 22904-4319, United States

[§]Department of Chemistry, The University of Alabama, Tuscaloosa, Alabama 35487-0336, United States

[∥]Institut für Chemie und Biochemie−Anorganische Chemie, Freie Universität Berlin, Fabeckstraße 34−36, D-14195 Berlin, Germany

Supporting Information

ABSTRACT: The compounds H_2ThSe and H_2USe were synthesized by the reaction of laser-ablated actinide metal atoms with H_2Se under cryogenic conditions following the procedures used to synthesize H_2AnX (An = Th, U; X = O, S). The molecules were characterized by infrared spectra in an argon matrix with the aid of deuterium substitution and electronic structure calculations at the density functional theory level. The main products, H_2ThSe and H_2USe, are shown to have a highly polarized actinide−selenium triple bond, as found for H_2AnS on the basis of electronic structure calculations. There is an even larger back-bonding of the Se with the An than found for the corresponding sulfur compounds. These molecules are of special interest as rare examples of multiple bonding of selenium to a metal, particularly an actinide metal.

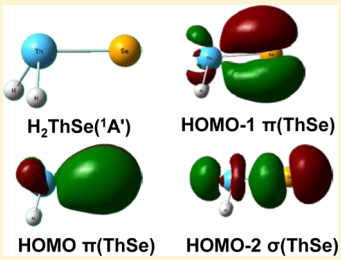

INTRODUCTION

Compounds of uranium and thorium with the light chalcogens oxygen and sulfur have been studied extensively in the bulk due to their importance in the nuclear fuel cycle.[1−4] Ligands containing soft donors are thought to be relevant for the separation of the later actinides from the lanthanides.[5,6] The infrared spectra of these molecules have been investigated by matrix isolation spectroscopy of the products generated from the reaction of laser-ablated metal atoms with oxygen or sulfur vapor. The experimental observations have been supported by electronic structure calculations, mostly at the density functional theory level.[7−11] Additional reactions of uranium and thorium atoms with H_2O, H_2O_2, H_2S, or methanol have also been reported.[12−17] However, very little is known about molecular actinide compounds containing selenium. Several uranium and thorium selenides have been studied in the bulk, but this work has not provided detailed information about the structures and bonding at the molecular level.[2,3] Most structures of uranium with chalcogenides have bridging chalcogenide ligands.[18−23] Recently, Hayton and his group have reported the synthesis of a terminal chalcogenide complex of uranium, $[K(18\text{-crown-6})][U(Se)(N(SiMe_3)_2)_3]$ (with a terminal U−Se bond complexed to the K^+crown).[24] The U−Se bond distance is 2.59 Å, which is shorter than the U−Se bond distance of 2.646 reported for $[Ph_3PCH_3][U(Se)(N(SiMe_3)_2)_3]$ by the same group.[25] The former value is the shortest that has been reported for a U−Se bond distance.[26]

Following the successful synthesis and characterization of H_2ThS and H_2US through the reaction of laser-ablated thorium and uranium atoms with H_2S under cryogenic conditions,[17] we have continued our studies of actinide−chalcogen bonding using H_2Se as the reagent. A natural bond order (NBO) analysis of the bonding in $XAnH_2$ with X = O and S and An = Th and U showed that there is more delocalization from the larger S 3p orbitals back-bonding to the metal than from the tighter O 2p orbitals.[17] Thus, the M−O bonding is more ionic than the M−S bonding, as would be expected from simple electronegativity considerations. The electron configuration on U is predicted to be $s^{0.4}d^{1.2}f^{2.6}$ for H_2UO and $s^{0.4}d^{1.7}f^{2.5}$ in H_2US in contrast to the f^2 expected for the formal +IV oxidation state. There is more 5f population on the U than expected from the formal oxidation state showing a role for the 5f orbitals in U bonding to the H and O or S. The NBO analysis suggests a highly polarized triple-bond character for both An−S bonds. There is more metal character in the US bonds than in the ThS bonds, and this additional character is mostly in the π bonds. There is more d character in the ThS π bonds and more f character in the US π bonds, consistent with the expected oxidation-state properties of the atoms. For example, atomic Th does not have any active f electrons in the ground state of the atom, and the Th in ThX_4 (X = F, Cl) behaves similarly to the group 4 transition metals.[27] We expect that this effect will be even more pronounced in the corresponding selenium compounds H_2ThSe and H_2USe due to the lower electronegativity of Se as compared to S. This work is of interest, as

Received: June 19, 2015
Published: September 29, 2015

DOI: 10.1021/acs.inorgchem.5b01383
Inorg. Chem. 2015, 54, 9761−9769

there are few species containing a multiple bond between selenium and a metal, particularly an actinide metal.

EXPERIMENTAL AND COMPUTATIONAL DETAILS

Gaseous H_2Se was synthesized by hydrolysis of Na_2Se or K_2Se with HCl (2 M) in a vacuum system. The effluent gas was dried through condensation over $CaCl_2$, then transferred into a glass bulb and stored in the dark to minimize decomposition. The glass bulb was mounted directly to the stainless steel matrix gas mixing system. Deuterium enrichment of H_2Se was accomplished by first exchanging the manifold of the mixing system with D_2O for several hours, then evacuating residual D_2O, and adding H_2Se for about 90 min, which produced HDSe and D_2Se with residual H_2Se. The D_2Se is generated by exchange between D_2O adsorbed on the surface of the manifold and H_2Se subsequently coadsorbed. The argon matrix spectrum of the resulting hydrogen selenide revealed an approximately 1:1:1 mixture of $H_2Se/HDSe/D_2Se$ as measured from their infrared band absorbances normalized by computed intensities. Allowing additional time for the latter exchange process failed to improve the enrichment. We did not have enough enriched selenide reagent to attempt additional reactions with more D_2O.

The H_2Se precursor mixed with excess argon was condensed onto a CsI window cooled to 10 K using a closed-cycle helium refrigerator (Sumitomo Heavy Industries, RDK-205D) supported in a vacuum chamber.[28] Uranium or thorium atoms were co-deposited with the argon/hydrogen selenide mixture following laser ablation from solid metal. The 1064 nm fundamental of a Nd:YAG laser (Continuum, Minilite II, 10 Hz repetition rate and 6 ns pulse width, laser energy about 25−40 mJ/pulse) was focused onto the rotating metal target through a hole in the cold window. Infrared spectra were recorded on a Bruker Vertex 70 spectrometer at 0.5 cm^{-1} resolution in the region between 4000 and 430 cm^{-1} using a liquid nitrogen cooled MCT detector. Far-IR spectra were recorded at 1 cm^{-1} resolution using a room-temperature LaDTGS detector. Matrix samples were irradiated by a mercury arc street lamp (Osram HQL 250) with the outer globe removed [radiation >220 nm, mostly UV−vis].

Calculations were performed at the B3LYP level because we have previously shown good agreement between these calculated frequencies and experimental values as well as with higher level CCSD(T) calculations for the H_2AnX (An = U, Th; X = O, S) molecules.[17] Calculations of the frequencies were done at the density functional theory level with the B3LYP functional using the Gaussian09 program.[29] In addition, CCSD(T) calculations[30−35] were performed to benchmark the results for H_2ThSe with the MOLPRO program.[36,37] The following triple-ζ basis sets were used: cc-pVTZ-PP for Th, U; aug-cc-pVTZ-PP for Se, and aug-cc-pVTZ for H.[38,39]

RESULTS AND DISCUSSION

Experimental Spectra. The infrared spectra of the reagent gas in argon show bands for H_2Se in the region 2290−2370 cm^{-1} and at 1033.3 cm^{-1}, which are in line with bands (2357.8 (ν_3, asymmetric stretch), 2344.5 (ν_1, symmetric stretch), 1034.2 (ν_2, bend)) reported in the literature.[40,41] The bending modes for HDSe and D_2Se are located at 899.8/895.3 and 741.2 cm^{-1}, respectively. The stretching modes of the Se−D bonds are in the 1650−1700 cm^{-1} region. These values or ranges are in line with reports in the literature (HDSe: 2352 (ν_3), 1691 (ν_1), 912 (ν_2); D_2Se: 1697 (ν_3), 1687 (ν_1), 741 (ν_2)).[41−43] In experiments with deuterated material weak absorptions for H_2O, HDO, and D_2O were also observed.

The reaction of laser-ablated thorium or uranium atoms with H_2Se in excess argon yielded two new and different infrared absorptions, shown in Figures 1 and 2, which are similar in appearance and relative intensities and just approximately 10 cm^{-1} higher than the band pairs assigned recently to H_2ThS and H_2US in solid argon.[15] It is straightforward to consider these bands to be the two metal dihydride stretching modes

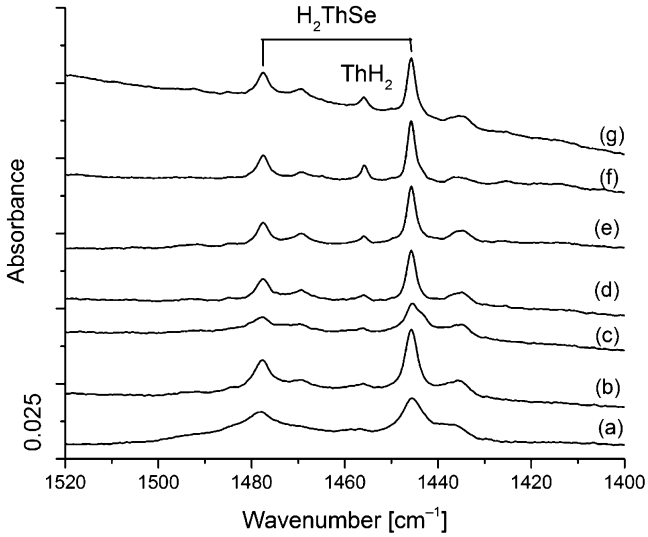

Figure 1. Infrared spectra of reaction products of laser-ablated thorium atoms with 2% H_2Se in argon recorded after (a) 55 min of deposition, (b) annealing to 26 K, (c) photolysis for 20 min, (d) annealing to 30 K, (e) annealing to 37 K, (f) annealing to 41 K, and (g) annealing to 46 K.

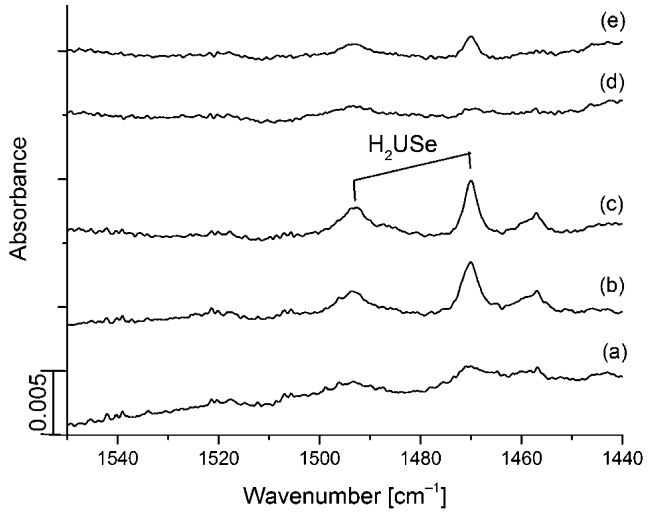

Figure 2. Reaction products of laser-ablated uranium atoms with 1% H_2Se in argon. (a) After 55 min of deposition, (b) annealing to 28 K, (c) annealing to 37 K, (d) photolysis for 20 min, (e) annealing to 38 K.

(symmetric and asymmetric) of the major stable *dihydride* reaction products H_2AnSe (An = Th, U). These new bands are observed after reaction during sample deposition at 1445.8 and 1477.5 cm^{-1} using thorium as the reagent (Figure 1a), and they increase in concert on annealing together with weaker satellite features at 1437 and 1470 cm^{-1} (Figure 1b), which are probably due to the major product perturbed by another reagent molecule in analogy with the $ThH_4(H_2)_x$ (x = 1−4) complexes.[44] The major bands decrease together by about 60% on photolysis (Figure 1c), but they increase again in concert on subsequent annealing cycles (Figure 1d−g). Clearly, these two bands behave as though they are due to the same new product molecule, as they increase together on annealing and decrease together on photolysis.

In addition, a band assigned toThH_2 was observed at 1455.8 cm^{-1}, in agreement with a prior study with a band at 1455.6

DOI: 10.1021/acs.inorgchem.5b01383
Inorg. Chem. 2015, 54, 9761−9769

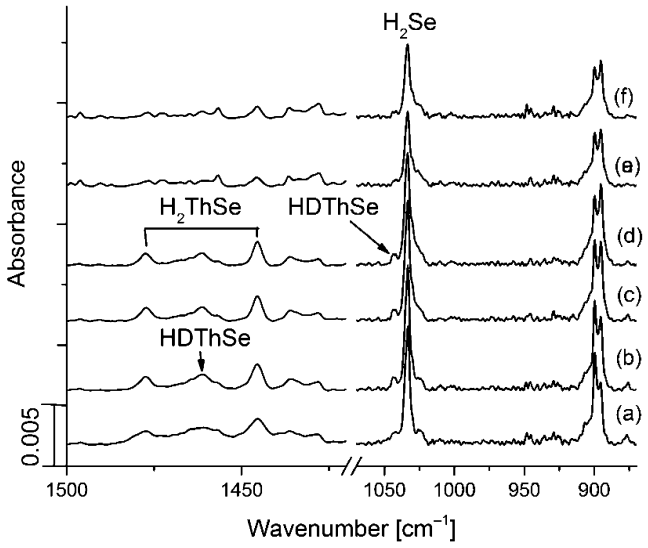

Figure 3. Reaction products of laser-ablated thorium atoms with 2% of a 1:1:1 mixture of H_2Se, HDSe, and D_2Se in argon. (a) After 50 min of deposition, (b) annealing to 27 K, (c) annealing to 34 K, (d) annealing to 39 K, (e) photolysis for 15 min, (f) annealing to 37 K.

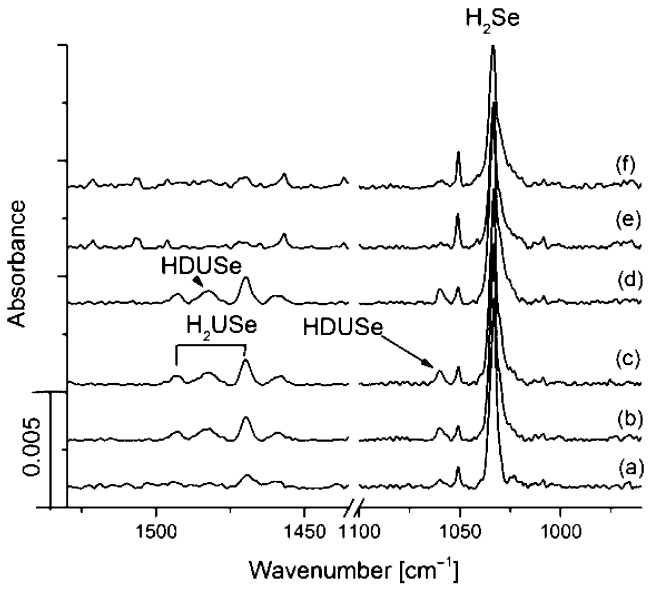

Figure 4. Reaction products of laser-ablated uranium atoms with 2% of a 1:1:1 mixture of H_2Se, HDSe, and D_2Se in argon. (a) After 50 min of deposition, (b) annealing to 37 K, (c) annealing to 35 K for 2 min, (d) annealing to 40 K, (e) photolysis for 15 min, (f) annealing to 41 K.

cm^{-1},[45] and the amount of ThH_2 increased here on annealing along with the major product. The sharp new absorption at 1445.8 cm^{-1} is just 1.0 cm^{-1} higher than the split band at 1444.8, 1443.3 cm^{-1} identified in earlier Th and H_2 reagent experiments.[5] This split band was assigned to the intense antisymmetric stretching mode of ThH_4, which is stable on photolysis,[44,45] in contrast to the present major product characterized by bands at 1445.8 and 1477.5 cm^{-1}, which show it to be photosensitive. The very weak band at 1484.8 cm^{-1} is probably due to ThH, previously observed at 1485.2 cm^{-1}, but we cannot be certain of this assignment.[45] We also measured the far-infrared spectra from 200 to 400 cm^{-1}, but we were not able to detect any weak-intensity metal−selenium stretching modes for either major product.

Two Th experiments were done using neon as the matrix gas, and spectra from the better of these are shown in Figure S1. Since the 4 K condensation temperature employed for Ne is much closer to the freezing point of Ne [24.5 K] than the 10 K temperature used for Ar is to its freezing point [84.0 K], Ne is condensed more slowly, and, for successful spectral observations, it is necessary to employ a substantially lower ablation laser energy. As a direct result, the two new product absorptions in Ne at 1464.5 and 1499.5 cm^{-1} are a factor of 10 weaker than the Ar matrix counterparts shown in Figure 1. Nevertheless, these Ne matrix absorptions increase on annealing to 10 K, decrease on UV photolysis, and increase on annealing to 11 K, which is analogous to their behavior in solid Ar. These Ne matrix bands are 18.7 and 22.0 cm^{-1} higher than the Ar matrix values, which compares very closely with the corresponding H_2ThS absorptions exhibiting 17 and 19 cm^{-1} blue shifts in solid Ne.[17]

The major uranium product has bands at 1470.0 and 1493.7 cm^{-1}, illustrated in Figure 2, which bracket UH_4 previously observed at 1483.6 cm^{-1}.[46] The behavior of these bands on annealing and photolysis is essentially the same as for the major thorium product. One other new band is observed in these experiments, at 1457.1 cm^{-1}. The 1457.1 cm^{-1} band shows a similar behavior on annealing and photolysis to the major product, so it is most likely due to a $H_2USe{\cdot}(H_2Se)_x$ complex in analogy with the thorium experiments. We were not able to detect any An−Se stretching modes in the far-infrared region where our spectral sensitivity is lower. Neon matrix experiments were not performed with U since U is less reactive than Th (the corresponding uranium sulfide bands were a factor of 4 weaker than the thorium counterparts),[17] and H_2Se is more difficult to manage owing to decomposition such that U products are unlikely to be observable in solid Ne. The anticipated blue shift from the Ar matrix absorptions in solid

Table 1. Observed Argon and Neon Matrix and Calculated Frequencies (cm^{-1}) for H_2ThSe ($^1A'$) in C_s Symmetry[a]

H_2ThSe		D_2ThSe	HDThSe		
ν expt[b]	ν (I) calc	ν (I) calc	ν expt	ν (I) calc	H_2ThSe mode assignment
1477.5/1499.5	1524.8 (379) [1530.1]	1080.7 (191)	1461.1	1503.8 (444)	Th−H sym str, a′
1445.8/1464.5	1481.5 (524) [1492.3]	1050.9 (266)	1043.7	1065.2 (236)	Th−H asym str, a″
	480.4 (125) [482.9]	344.9 (80)		429.8 (104)	ThH_2 bend, a′
	380.5 (12) [383.7]	271.2 (5)		299.9 (35)	H−Th−Se asym bend, a″
	377.9 (123) [374.0]	301.3 (46)		359.5 (68)	H−Th−Se bend + Th−Se str a′
	281.0 (4) [283.3]	248.4 (15)		258.4 (7)	Th−Se str + H−Th−Se bend, a′

[a]Frequencies calculated in the harmonic approximation at the B3LYP level with the following basis sets: aug-cc-pVTZ on H, aug-cc-pVTZ-PP on Se, and cc-pVTZ-PP on Th. Calculated intensities in km mol^{-1} are given in parentheses. The CCSD(T) frequencies are given in brackets for H_2ThSe. [b]Neon matrix frequencies are after the slash. Estimated gas-phase frequencies are 1475 and 1505 ± 10 cm^{-1}.

DOI: 10.1021/acs.inorgchem.5b01383
Inorg. Chem. 2015, 54, 9761−9769

Table 2. Observed and Calculated Frequencies for H_2US ($^3A''$) in C_s Symmetry[a]

H_2USe		D_2USe	HDUSe		
ν expt	ν (I) calc	ν (I) calc	ν expt	ν (I) calc	H_2ThSe mode assignment
1493.7	1532.6 (440)	1086.3 (223)	1482.2	1516.4 (483)	U−H sym str, a′
1470.0	1499.3 (536)	1063.5 (272)	1060.0	1074.6 (252)	U−H asym str, a″
	486.6 (67)	347.1 (42)		423.9 (60)	UH_2 bend, a′
	344.5 (164)	303.3 (62)		331.3 (116)	H−U−Se bend + U−Se str, a′
	309.1 (6)	220.2 (1)		274.6 (2)	H−U−Se asym bend, a″
	256.3 (9)	206.4 (32)		212.7 (21)	U−Se str + H−U−Se bend, a′

[a]Frequencies calculated in the harmonic approximation at the B3LYP level with the following basis sets: aug-cc-pVTZ on H, aug-cc-pVTZ-PP on Se, and cc-pVTZ-PP on U. Calculated intensities in km mol^{-1} are given in parentheses. We estimate the gas-phase frequencies for H_2USe to be 1500 and 1525 ± 10 cm^{-1}.

Table 3. B3LYP-Optimized Structural Parameters for the H_2MSe (M = Th, U) Molecular Ground States

property	H_2ThSe (C_s − $^1A'$)[a]	H_2USe (C_s − $^3A''$)
r(M−Se), Å	2.534 [2.541]	2.484
r(M−H), Å	2.059 [2.068]	1.999
∠Se−M−H, deg	101.2 [100.8]	101.7
∠H−M−H, deg	101.1 [130.5]	99.8

[a]Values in brackets are CCSD(T).

Table 4. CCSD(T)/aug-cc-pvTZ Values for the ThSe and USe Diatomic Molecular Ground States[a]

property	^{1}ThSe	^{5}USe
r(Th−X), Å	2.500 (2.530)	2.526 (2.518)
Th−X str. (harmonic), cm^{-1}	306.0 (308.5)	284.6 (274.3)
anharmonicity, cm^{-1}	0.43	0.77
ΔE, kJ mol^{-1}	53.2 (S−T)[b]	28.5 (Q−T)[c]

[a]Data obtained from a five-point fit. B3LYP values are in parentheses. [b]Singlet−triplet energy splitting. [c]Quintet-triplet energy splitting.

Table 5. CCSD(T) Reaction Energies and Heats of Formation at 298 K in kJ mol^{-1}

molecule	ΔH_f(298 K)	reaction	ΔH_{rxn}(298 K)
H_2ThO	−79.1	$ThO_2 + H_2O \rightarrow H_2ThO + O_2$	598.3
H_2ThS	183.3	$ThO_2 + H_2S \rightarrow H_2ThS + O_2$	639.3
H_2ThSe	205.4	$ThO_2 + H_2Se \rightarrow H_2ThSe + O_2$	610.4
	205.9	$H_2ThO + H_2Se \rightarrow H_2ThSe + H_2O$	12.6
	215.9	$H_2ThS + H_2Se \rightarrow H_2ThSe + H_2S$	−18.4
H_2UO	−18.8	$UO_3 + H_2 \rightarrow H_2UO + O_2$	776.1
H_2US	258.6	$H_2UO + H_2S \rightarrow H_2US + H_2O$	56.1
H_2USe	305.9	$H_2US + H_2Se \rightarrow H_2USe + H_2S$	−3.8
	333.0	$H_2UO + H_2Se \rightarrow H_2USe + H_2O$	79.5
H_2O	−241.8[d]		
H_2S	−20.5 ± 0.8[d]		
H_2Se	29.7[c]		
Th	602.1 ± 5.9[a]		
U	533.0 ± 8.4[a]		
ThO_2	−435.6 ± 12.6[b]		
UO_3	−796.7 ± 10[b]		

[a]Reference 54. [b]Reference 55. [c]Reference 56. [d]Reference 57.

Ne for H_2USe is most probably close to that observed for H_2US, namely, 20−22 cm^{-1}.

In addition to the experiments with H_2Se, we also investigated isotopic shifts of the product spectra on deuterium substitution. Several experiments with mixtures of H_2Se, HDSe, and D_2Se were carried out. The H_2Se/HDSe/D_2Se sample employed was approximately 1:1:1 as determined by comparison of the relative band intensities with calculated harmonic intensities; see Figure S2 in the Supporting Information. Many attempts to increase the amount of D_2Se such as longer exchange times failed. Due to the low content of D_2Se and the overall low IR band intensities of the desired products, we were not able to detect fully deuterated products. However, mixed isotope products were identified in these experiments, as shown in Figures 3 and 4, which confirm the present identifications and assignments.

Weaker new bands for the mixed isotopic product with Th were found at 1461.1 and 1043.7 cm^{-1}. These bands show the same behavior on first annealing and photolysis as the bands of the Th hydride product. However, the re-formation on annealing of either the hydrogenated product or the mixed isotope product after UV photolysis was difficult to observe in the mixed H/D experiments. Similar experiments have been carried out with laser-ablated uranium atoms and mixed isotopic reagents, resulting in weak new bands for the mixed isotope product with U at 1482.2 and 1060.0 cm^{-1}.

The test for the uncoupled Th−H stretching mode of HDThSe is that it should be the average of the coupled a′ (symmetric) and a″ (antisymmetric) Th−H stretching modes observed for H_2ThSe: this average (1461.6 cm^{-1}) is in excellent agreement with the observed 1461.1 cm^{-1} mixed isotopic band. This observation of a *single* mixed isotopic band at the median between *two* fully hydrogenated symmetric and antisymmetric stretching counterparts confirms the identification of the major product as a dihydride. The proximity of the subject 1445.8 and 1477.5 cm^{-1} bands to those mentioned above for ThH_2 and ThH_4 supports their origin as a new thorium dihydride bearing molecule, and their appearance just 10 cm^{-1} above the two Th−H stretching modes for H_2ThS invites their assignment to H_2ThSe.

This identification is confirmed by our calculated electronic structure frequencies for H_2ThSe and HDThSe in Table 1. First, the average calculated value is 1503.2 cm^{-1} for the two stretches for H_2ThSe, and the value for HDThSe is 1503.8 cm^{-1}. The same rationale can also be applied to the Th−D stretching mode for HDThSe, but we were not able to observe the a′ symmetric and a″ antisymmetric stretching modes for D_2ThSe. The expected band positions can be predicted from the H_2ThSe counterparts when divided by the H/D frequency

DOI: 10.1021/acs.inorgchem.5b01383
Inorg. Chem. 2015, 54, 9761−9769

Table 6. B3LYP Natural Electron Configurations on Th and U and Charges on All Elements[a]

molecule	$M(7s)^b$	$M(7p)^b$	$M(6d)^b$	$M(5f)^b$	$q(M)^b$	$q(E)^c$	$q(H)$
ThO	1.84	0.10	0.71	0.34	1.10	−1.10	
ThS	1.80	0.06	1.18	0.24	0.77	−0.77	
ThSe	1.79	0.06	1.29	0.21	0.68	−0.68	
UO	0.93	0.07	0.88	3.10	1.07	−1.07	
US	0.95	0.06	1.03	3.10	0.88	−0.88	
USe	0.99	0.06	1.04	3.09	0.84	−0.84	
H_2ThO	0.36	0.10	1.28	0.39	1.99	−1.02	−0.48
H_2ThS	0.42	0.08	1.72	0.31	1.56	−0.69	−0.43
H_2ThSe	0.44	0.08	1.79	0.28	1.48	−0.62	−0.43
H_2UO	0.35	0.10	1.21	2.61	1.81	−0.86	−0.47
H_2US	0.43	0.10	1.66	2.54	1.32	−0.56	−0.38
H_2USe	0.46	0.10	1.70	2.52	1.26	−0.51	−0.38

[a]Units of electrons. [b]M = Th or U. [c]E = O, S, or Se.

Table 7. Calculated B3LYP NBO Analysis for H_2MSe

bond	M pop %	M %7s	M %6d	M %5f	H/Se pop %	H/Se %s	Se %p
				H_2ThSe			
Th−Se π	21		80	15	79		95
Th−Se π	20		81	16	80		100
Th−Se σ	27	23	66	8	73	14	86
Th−H σ	29	30	59	8	71	100	
				H_2MSe ($^3A''$) α			
U−Se π	25		68	27	75		97
U−Se π	28		53	44	72		100
U−Se σ	28	24	65	11	72	13	87
U−H σ	33	26	52	19	67	100	
U *lp*	100			97			
U *lp*	100			100			
				H_2MSe ($^3A''$) β			
U−Se π	19		71	25	81		99
U−Se π	19		68	28	81		100
U−Se σ	26	22	60	18	74	17	83
U−H σ	30	28	55	13	70	100	

ratios, 1.4021 and 1.3992, observed for the analogous modes of H_2Th and D_2Th.[45] This gives 1033.3 and 1053.8 cm^{-1} values and a 1043.6 cm^{-1} average that is in excellent agreement with the 1043.7 cm^{-1} band observed for the Th−D stretching mode for HDThSe. Again, our electronic structure calculations verify this relationship: the average calculated a′ and a″ frequency for D_2ThSe is 1065.8 cm^{-1}, and the calculated Th−D stretching mode for HDThSe is 1065.2 cm^{-1}. The fact that the lower and more intense band of D_2ThSe is probably underneath the 1033.3 cm^{-1} band for the H_2Se precursor and the upper band has a quite low intensity provide possible reasons that D_2ThSe could not be detected in this experiment.

Bands for D_2USe are estimated at 1049.6 and 1066.0 cm^{-1} from the H_2USe modes observed at 1470.0 and 1493.7 cm^{-1}, and the H/D isotopic ratios are 1.4005 and 1.4012 for the two modes of H_2U and D_2U;[46] however, these bands were not observed here. However, the average frequencies of the pure isotopic product species, 1481.9 cm^{-1} from observed H_2USe modes and 1057.8 cm^{-1} from estimated D_2USe modes, and the computed frequencies in Table 2 support our 1482.2 and 1060.0 cm^{-1} assignment to the U−H and U−D stretching modes for HDUSe. The sharp weak band at 1050.9 cm^{-1}, which increases markedly on full arc photolysis, is due to NUN from the reaction of U* with a trace of N_2 impurity in the vacuum system, which is detected in most of our experiments with laser-ablated uranium.[17,46,47] This observation confirms that the experimental laser ablation conditions for U atoms are appropriate for the formation and spectroscopic detection of new molecules.

Computational Results. The harmonic frequencies and intensities computed at the DFT/B3LYP level are given in Tables 1 and 2. The good correspondence between the experimental and calculated values for the major product bands of H_2ThSe and H_2USe provides confirmation of the above assignments as belonging to these molecules. For the thorium product in the $^1A'$ ground state, the more intense antisymmetric stretching a″ mode is computed to be 2.5% higher than observed, and the less intense symmetric stretching a′ mode is computed to be 3.2% higher than observed: similar differences were found for the sulfide analogue H_2ThS.[17] This is to be expected when comparing the experimental anharmonic frequencies with the calculated harmonic frequencies, especially for those involving hydrogen.[17] We further validated the use of DFT for the harmonic frequencies by performing CCSD(T) calculations with the same basis sets on H_2ThSe (Table 1) and showed that the DFT and CCSD(T) values are within 11 cm^{-1} of each other. We estimate the gas-phase frequencies for H_2ThSe to be 1475 ± 10 and 1505 ± 10 cm^{-1} based on the experimental values being 2% too low due to Ar matrix effects, consistent with the Ne matrix shifts.

DOI: 10.1021/acs.inorgchem.5b01383
Inorg. Chem. 2015, 54, 9761−9769

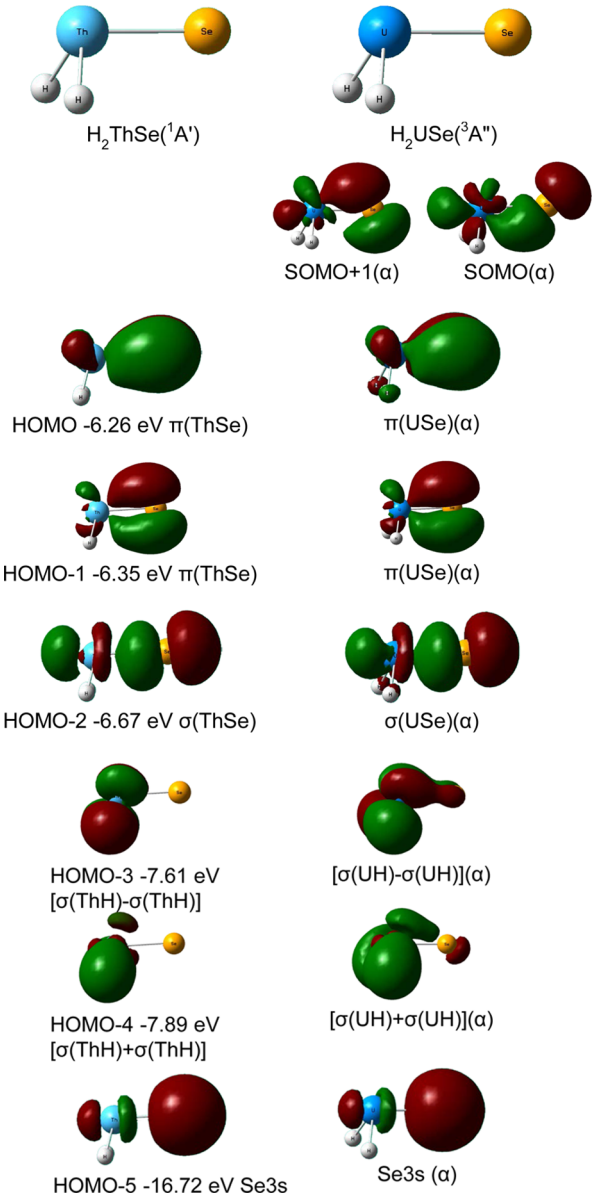

Figure 5. Comparison of σ and π molecular orbitals calculated for the for H_2ThSe and H_2USe molecules using the B3LYP functional with an iso-electron density counter of 0.04 e/au^3. Alpha spin orbitals are plotted for the U $^3A''$ species, and doubly occupied orbitals are plotted for the Th $^1A'$ species.

For the uranium product in the $^3A''$ ground state, the computed DFT frequencies are slightly closer to experiment, 2.0% and 2.6% higher than the observed values. The triplet ground state for H_2USe is $^3A''$ derived from a $(a')^1(a'')^1$ occupancy. There are two slightly higher energy triplets with A′ symmetry derived from the $(a')^1(a')^1$ occupancy (10.5 kJ mol^{-1}) and $(a'')^1(a'')^1$ occupancy (14.6 kJ mol^{-1}) for the vertical energies at the $^3A''$ geometry. (We were unable to optimize the geometry for H_2USe at the CCSD(T) level due to wave function convergence issues in the optimization, nor were we able to converge the two $^3A'$ states at the DFT level during the geometry optimization.) We estimate the gas-phase frequencies for H_2USe to be 1500 ± 10 and 1525 ± 10 cm^{-1} based on the experimental values being 2% too low due to Ar matrix effects. The DFT gas-phase frequencies are in good agreement with these estimated frequencies derived from the Ar matrix values.

In order to exclude the possibility of another species that might be the carrier of the 1457.1 cm^{-1} band, we also optimized the structure of HSeUH, which is a quintet. It is 27.6 kJ mol^{-1} above the triplet ground state of H_2USe. It has a planar cis structure with r(Se−H) = 1.484 Å, r(U−H) = 2.042 Å, r(Se−U) = 2.786 Å, ∠H−Se−U = 79.8°, and ∠H−U−Se = 104.6°. The calculated U−H stretching frequency is 1423.7 cm^{-1} (393 km mol^{-1}). Taking the average shift of about 30−40 cm^{-1} between calculation and experiment into account, the expected experimental frequency is in the 1375−1390 cm^{-1} range. Thus, we do not assign the 1457.1 cm^{-1} band to HSeUH. The large predicted difference between the U−H stretches in H_2USe and HSeUH are due to different isomeric structures with different formal uranium oxidation states. This is in contrast to what is observed for CUO, where the spin state was found to depend on whether the molecule is in an Ar or Ne matrix with significant shifts in the Ar matrix due to interactions of the CUO with the Ar, leading to a change in the spin state.[48] As noted above, when estimates are taken into account for the Ar matrix shifts, there is good agreement with the values predicted for the gas-phase molecule, so the matrix is not affecting the basic structure of the molecule.

For H_2ThSe, the two lowest frequency modes are combinations of the Th−Se stretch and the H−Th−Se symmetric bend, with more bend in the higher frequency mode and more stretch in the lower frequency mode. The antisymmetric bend and symmetric bend plus stretch modes are almost degenerate in H_2ThSe. For H_2USe, the makeup of these low frequency modes is somewhat different. Again, the U−Se stretch and the symmetric H−U−Se bend are coupled. For H_2USe, the asymmetric H−U−Se bend is between the two low-energy a′ modes, and there is no approximate accidental degeneracy of an a′ and a″ mode as in H_2ThSe. The comparison of the dideuterated with the dihydrogen low-energy modes provides additional insights into the amount of M−Se stretch mixed with the symmetric H−M−Se bend. For the higher frequency mode with more bend, the H_2:D_2 ratio is 1.254 for M = Th and 1.14 for U as compared to the ratio of 1.414 expected from the masses. For the lower frequency mode, the ratio is 1.13 for Th and 1.24 for U, showing that there is more bend in the low-frequency mode for U and more bend in the high-frequency mode for Th. For comparison, the H_2M bend ratios are 1.393 for Th and 1.402 for U, and the a″ HMSe bend ratios are 1.403 for Th and 1.404 for U, showing the expected isotopic mass ratios.

We also used the numerical differentiation of analytically derived normal modes available in Gaussian09 to calculate the anharmonic corrections to the harmonic frequencies at the same DFT level used to calculate the harmonic frequencies.[49−52] The default displacement of 0.025 Å was used in the numerical differentiation. The results (Supporting Information) show that the anharmonic corrections to the Th−H and U−H stretching frequencies are small (<6 cm^{-1}), so that any further differences between the calculations and experiment are due to errors in the prediction of the harmonic frequencies. There are larger anharmonic effects on the bends with corrections of 20 to 35 cm^{-1}. For H_2ThSe, most of the anharmonic corrections to the bends are positive, increasing the frequency. For H_2USe, the anharmonic corrections for most of the bends are negative, with only one showing an increased frequency due to anharmonicity.

DOI: 10.1021/acs.inorgchem.5b01383
Inorg. Chem. 2015, 54, 9761−9769

The optimized molecular structure parameters for H_2MSe are given in Table 3. Both molecules are nonplanar. The U−Se and U−H bond distances are shorter than the corresponding Th−Se and Th−H bond distances. The U−H stretching frequencies are higher than the Th−H stretching frequencies, consistent with the shorter bond distances for the uranium compound. The bond angles are essentially the same for uranium and thorium compounds. The calculated U−Se bond distance of 2.48 Å is ∼0.1 Å shorter than the shortest known U−Se bond reported by Hayton and co-workers.[24] The shorter value for the simple H_2USe molecule is not surprising given that the Se in the complex reported by Hayton is complexed to a K^+(18-crown-6), which will lengthen the U−Se bond. The calculated values for the Th−Se and U−Se bond lengths of 2.53 and 2.48 Å, respectively, are slightly longer than the respective sum of the double-bond lengths calculated from the r_2 covalent radii of Pyykkö and Atsumi[33] of 2.50 and 2.41 Å.

The geometry parameters and vibrational frequencies for diatomic MSe are given in Table 4 at the CCSD(T) and B3LYP levels. The open-shell calculations were performed at the R/UCCSD(T) level starting with restricted open-shell Hartree−Fock orbitals and a spin-unrestricted CCSD(T).[33−35] ThSe is predicted to be a ground-state singlet, with the triplet state 54.4 kJ mol^{-1} higher in energy. The ground state of USe is a quintet state. The spatial state description is more difficult to assign due to the use of only C_{2v} symmetry and the lack of spin−orbit corrections. A triplet state is 29.3 kJ mol^{-1} higher in energy. There is reasonable agreement between the CCSD(T) and B3LYP values. ThSe is predicted to have a shorter bond distance at the CCSD(T) level than USe, and the reverse is predicted at the B3LYP level. The difference between the B3LYP and CCSD(T) results is small, as all of the calculated diatomic bond distances are within 0.03 Å of each other. Surprisingly, the stretching frequencies have the same order at both computational levels, with the ThSe stretch predicted to be higher than the USe stretch.

The heats of formation for H_2MSe were calculated at the CCSD(T) level with the various triple-ζ basis sets described above and available experimental data using the reactions in Table 5.[54−57] We include the data needed to calculate the values for H_2MO and H_2MS as well, as these were used in the calculation of the heats of formation for H_2MSe. There is good agreement for the heats of formation from the various reaction energies for H_2ThSe, giving an average value of $\Delta H_f(H_2ThSe, 298\ K) = 209.2$ kJ mol^{-1}. There is a larger variation for the heat of formation of H_2USe, with the average value of $\Delta H_f(H_2USe, 298\ K) = 303.8$ kJ mol^{-1}. These heats of formation are probably good to ±15 kJ/mol considering the errors in the experimental heats of formation and in the calculations.

The heats of formation were then used to calculate the following reaction energies in kJ mol^{-1}.

$$Th + H_2O \rightarrow H_2ThO \quad \Delta H_{rxn}(298\ K) = -439 \qquad (1)$$

$$Th + H_2S \rightarrow H_2ThS \quad \Delta H_{rxn}(298\ K) = -398 \qquad (2)$$

$$Th + H_2Se \rightarrow H_2ThSe \quad \Delta H_{rxn}(298\ K) = -423 \qquad (3)$$

$$U + H_2O \rightarrow H_2UO \quad \Delta H_{rxn}(298\ K) = -310 \qquad (4)$$

$$U + H_2S \rightarrow H_2US \quad \Delta H_{rxn}(298\ K) = -255 \qquad (5)$$

$$U + H_2Se \rightarrow H_2USe \quad \Delta H_{rxn}(298\ K) = -243 \qquad (6)$$

The reactions are all exothermic, with the Th reactions more exothermic than the U reactions. The Th reactions do not show any periodic trends, whereas the U reactions show a decrease in the reaction energy from O to Se.

We performed a natural population analysis (NPA) based on the NBOs[58−62] calculated at the B3LYP level of theory for H_2MSe to better understand the bonding in these molecules. The results are shown in Table 6 together with our prior results for H_2MO and H_2MS as well as the corresponding diatomics.

The ThX diatomics have ∼1.8 electrons in the 7s on the Th. As the atom changes from O to S to Se, the 6d population increases from 0.7 to 1.3 e and the 5f population decreases from 0.34 to 0.21 e. Thus, the dominant electron configuration is $\sim 7s^2 6d^1$ for ThX. The ionicity of the bonding decreases as X changes from O to Se, consistent with the decrease in electronegativity going down the column. The UX diatomics have a different electron configuration that can be described as $\sim 7s^1 6d^1 5f^3$. The ionicity of the bonding also decreases as X is changed from O to Se. In both cases, the metal has about one electron on it. In ThX, the electron transferred to the X comes from the 6d and for UX from the 7s.

For H_2ThX, the ionicity decreases from O to Se, as in the diatomics with Th being substantially more ionic in H_2ThX than in ThX. There is less than 0.5 e in the 7s, and the population in the 7s increases from O to Se. The 6d population increases from 1.3 e for H_2ThO to 1.8 e for H_2ThSe. The 5f population is in the range of 0.4 to 0.3 e. The corresponding H_2UX compounds show similar populations in the 7s and 6d and ∼2.5 e in the 5f. The H_2UX are less ionic than the H_2ThX. The electron configurations for H_2ThSe and H_2USe are $s^{0.4}d^{1.8}f^{0.3}$ and $s^{0.5}d^{1.7}f^{02.5}$ and show close similarity to the bonding in the H_2MS compounds previously described.[17]

We also analyzed the NBOs for H_2ThSe and H_2USe, as shown in Table 7. The NBO analysis is essentially the same as that for H_2MS.[17] There are two very polarized Th−Se π bonds with about 80% population on the Se p orbitals. In both π bonds, 80% of the small Th population is in the 6d. The Th−H and Th−Se σ bonds have about 70% population on the H or Se. There is little population in the 5f in the σ bonds with two-thirds of the Th population found in the 6d and 20−30% of the population in the 7s. Very similar results for the bonding orbitals are found for the U in H_2USe for the α and β electrons. As expected, the two unpaired electrons are 5f orbitals on the U.

The Kohn−Sham orbitals are shown in Figure 5. The three highest occupied molecular orbitals for H_2ThSe show that the bonding for the Th−Se can be described as a σ bond plus two π-type bonds, which are highly localized on the Se, just as found in H_2ThS. The bonding for the doubly occupied orbitals is essentially the same in H_2USe. The two singly occupied orbitals in H_2USe are 5f orbitals that are partially delocalized on the Se. The two σ U−H orbitals show some delocalization to the Se, but no such delocalization is predicted for the Th−H σ orbitals. This is very similar to what was predicted for H_2ThS and H_2US. However, the back-bonding in H_2ThSe and H_2USe and therefore also the stabilization of the An−H bonds are stronger than in the sulfur and oxygen species, as the higher An−H stretching frequencies compared to H_2AnO and H_2AnS show.

CONCLUSIONS

We report the successful synthesis of H_2ThSe and H_2USe in an Ar matrix and their characterization by IR spectroscopy. Together with the dihydrogen compounds, the mixed H/D

DOI: 10.1021/acs.inorgchem.5b01383
Inorg. Chem. 2015, 54, 9761−9769

compounds HDThSe and HDUSe were observed by using a mixture of $H_2Se/HDSe/D_2Se$, although the dideuterated compounds were not observed. Comparison of the infrared spectra obtained in a Ne matrix supports the assignment of the argon matrix vibrational bands to H_2ThSe. Our experimental results for the frequencies and their assignments are confirmed by quantum chemical calculations at the DFT level, with the Th results further benchmarked at the CCSD(T) level. An NPA and NBO analysis shows that the bonding in H_2ThSe and H_2USe is quite similar to the sulfur analogues. The higher An−H stretching frequencies in the Se compounds than in the S compounds provide experimental evidence for a slightly stronger back-bonding from the Se-4p orbitals compared to the S-3p orbitals, consistent with the lower electronegativity of the Se as compared to S. This is consistent with a decrease in the ionic character of the M−Se bond. On the basis of the NBOs, the M−Se bond can be described as a highly polarized triple bond, like the bond between Th and U with S in H_2ThS and H_2US. The calculated bond distance for U−Se in H_2USe represents the shortest U−Se distance known. Even the simple analysis in terms of the r_2 double-bond radii suggests that the M−Se bonds are close to double bonds. The fact that the M−Se bond is less ionic than the M−S bond, yet there is comparable bonding in terms of the NBO analysis, also suggests that there is some type of multiple bonding in the M−Se bond in H_2MSe. The combined experimental and computational results thus provide strong evidence for multiple bonding between An and Se. We do note that there are many types of analyses that can be used to describe the bond between any two atoms and that the description of the bond does depend on how it is analyzed.

■ ASSOCIATED CONTENT

Supporting Information

The Supporting Information is available free of charge on the ACS Publications website at DOI: 10.1021/acs.inorgchem.5b01383.

Complete citations for refs 29 and 36, infrared spectra of a 1% $H_2Se/HDSe/D_2Se$ mixture in argon, energies used to predict the heats of formation, anharmonic frequencies, and infrared intensities for H_2MSe, and Cartesian coordinates for H_2ThSe and H_2USe (PDF)

■ AUTHOR INFORMATION

Corresponding Authors

*E-mail (L. Andrews): lsa@virginia.edu.
*E-mail (D. A. Dixon): dadixon@bama.ua.edu.
*E-mail (S. Riedel): sriedel@fu-berlin.de.

Notes

The authors declare no competing financial interest.

■ ACKNOWLEDGMENTS

We gratefully acknowledge financial support from Fond der Chemischen Industrie (T.V.-S.) and from the Department of Energy, Office of Science, Basic Energy Sciences Heavy Element Program, for the computational studies (D.A.D.). D.A.D. thanks the Robert Ramsay Fund of The University of Alabama for partial support. L.A. acknowledges retirement funds from TIAA.

■ REFERENCES

(1) Wells, A. F. *Structural Inorganic Chemistry*, 4th ed.; Oxford University Press: New York, 1975.
(2) Graham, J.; McTaggart, F. K. *Aust. J. Chem.* **1960**, *13*, 67.
(3) Sergushin, N. P.; Nefedov, V. I.; Rozanov, I. A.; Slovyanskikh, V. K.; Gracheva, N. V. *Zh. Neorg. Khim.* **1977**, *22*, 856−8.
(4) Grønvold, F. *J. Inorg. Nucl. Chem.* **1955**, *1*, 357−370.
(5) Jensen, M. P.; Bond, A. H. *J. Am. Chem. Soc.* **2002**, *124*, 9870−9877.
(6) Ingram, K. I. M.; Tassell, M. J.; Gaunt, A. J.; Kaltsoyannis, N. *Inorg. Chem.* **2008**, *47*, 7824−7833.
(7) Liang, B.; Andrews, L.; Ismail, N.; Marsden, C. J. *Inorg. Chem.* **2002**, *41*, 2811−2813.
(8) Liang, B.; Andrews, L. *J. Phys. Chem. A* **2002**, *106*, 4038−4041.
(9) Andrews, L.; Wang, X.; Liang, B.; Ruipérez, F.; Infante, I.; Raw, A. D.; Ibers, J. A. *Eur. J. Inorg. Chem.* **2011**, *2011*, 4457−4463.
(10) Zhou, M.; Andrews, L.; Ismail, N.; Marsden, C. *J. Phys. Chem. A* **2000**, *104*, 5495−5502.
(11) Hunt, R. D.; Andrews, L. *J. Chem. Phys.* **1993**, *98*, 3690−3696.
(12) Liang, B.; Andrews, L.; Li, J.; Bursten, B. E. *J. Am. Chem. Soc.* **2002**, *124*, 6723−6733.
(13) Liang, B.; Hunt, R. D.; Kushto, G. P.; Andrews, L.; Li, J.; Bursten, B. E. *Inorg. Chem.* **2005**, *44*, 2159−2168.
(14) Wang, X.; Andrews, L. *Phys. Chem. Chem. Phys.* **2005**, *7*, 3834−3838.
(15) Wang, X.; Andrews, L.; Li, J. *Inorg. Chem.* **2006**, *45*, 4157−4166.
(16) Gong, Y.; Andrews, L. *Inorg. Chem.* **2011**, *50*, 7099−7105.
(17) Wang, X.; Andrews, L.; Thanthiriwatte, K. S.; Dixon, D. A. *Inorg. Chem.* **2013**, *52*, 10275−10285.
(18) Brennan, J. G.; Andersen, R. A.; Zalkin, A. *Inorg. Chem.* **1986**, *25*, 1761−1765.
(19) Avens, L. R.; Barnhart, D. M.; Burns, C. J.; McKee, S. D.; Smith, W. H. *Inorg. Chem.* **1994**, *33*, 4245−4254.
(20) Gaunt, A. J.; Scott, B. L.; Neu, M. P. *Inorg. Chem.* **2006**, *45*, 7401−7407.
(21) Spencer, L. P.; Yang, P.; Scott, B. L.; Batista, E. R.; Boncella, J. M. *Inorg. Chem.* **2009**, *48*, 11615−11623.
(22) Lam, O. P.; Heinemann, F. W.; Meyer, K. *Chemical Science* **2011**, *2*, 1538−1547.
(23) Brown, J. L.; Wu, G.; Hayton, T. W. *Organometallics* **2013**, *32*, 1193−1198.
(24) Smiles, D. E.; Wu, G.; Hayton, T. W. *Inorg. Chem.* **2014**, *53*, 10240−10247.
(25) Brown, J. L.; Fortier, S.; Lewis, R. A.; Wu, G.; Hayton, T. W. *J. Am. Chem. Soc.* **2012**, *134*, 15468−15475.
(26) Hayton, T. W. *Chem. Commun.* **2013**, *49*, 2956−2973.
(27) Thanthiriwatte, K. S.; Vasiliu, M.; Battey, S. R.; Lu, Q.; Peterson, K. A.; Andrews, L.; Dixon, D. A. *J. Phys. Chem. A* **2015**, *119*, 5790−5803.
(28) Schloeder, T.; Vent-Schmidt, T.; Riedel, S. *Angew. Chem., Int. Ed.* **2012**, *51*, 12063−12067.
(29) Frisch, M. J.; Trucks, G. W.; Schlegel, H. B.; Scuseria, G. E.; Robb, M. A.; Cheeseman, J. R.; Scalmani, G.; Barone, V.; Mennucci, B.; Petersson, G. A.; et al. *Gaussian 09*, Revision C.01; Gaussian, Inc.: Wallingford, CT, 2009.
(30) Bartlett, R. J.; Musial, M. *Rev. Mod. Phys.* **2007**, *79*, 291−352.
(31) Purvis, G. D., III; Bartlett, R. J. *J. Chem. Phys.* **1982**, *76*, 1910−18.
(32) Raghavachari, K.; Trucks, G. W.; Pople, J. A.; Head-Gordon, M. *Chem. Phys. Lett.* **1989**, *157*, 479−83.
(33) Watts, J. D.; Gauss, J.; Bartlett, R. J. *J. Chem. Phys.* **1993**, *98*, 8718−33.
(34) Knowles, P. J.; Hampel, C.; Werner, H. J. *J. Chem. Phys.* **1993**, *99*, 5219−27.
(35) Deegan, M. J. O.; Knowles, P. J. *Chem. Phys. Lett.* **1994**, *227*, 321−6.
(36) Werner, H.-J. Knowles, P. J.; Knizia, G.; Manby, F. R.; Schütz, M.; Celani, P.; Korona, T.; Lindh, R.; Mitrushenkov, A.; Rauhut, G.;

DOI: 10.1021/acs.inorgchem.5b01383
Inorg. Chem. 2015, 54, 9761−9769

et al. *MOLPRO*, version 2012.1, a package of ab initio programs. See http://www.molpro.net, 2012.
(37) Werner, H.-J.; Knowles, P. J.; Knizia, G.; Manby, F. R.; Schuetz, M. *Wiley Interdiscip. Rev. Comput. Mol. Sci.* **2012**, *2*, 242−253.
(38) Kendall, R. A.; Dunning, T. H.; Harrison, R. J. *J. Chem. Phys.* **1992**, *96*, 6796−6806.
(39) Peterson, K. A. *J. Chem. Phys.* **2015**, *142*, 074105/1−074105/14.
(40) Cameron, D. M.; Sears, W. C.; Nielsen, H. H. *J. Chem. Phys.* **1939**, *7*, 994−1002.
(41) Shimanouchi, T. *Tables of Molecular Vibrational Frequencies Consolidated Vol. I*; National Bureau of Standards, 1972; pp 1−160.
(42) Ulenikov, O. N.; Onopenko, G. A.; Tyabaeva, N. E.; Burger, H.; Jerzembeck, W. *J. Mol. Spectrosc.* **1999**, *197*, 100−113.
(43) Ulenikov, O. N.; Burger, H.; Jerzembeck, W.; Onopenko, G. A.; Zhabina, E. A.; Petrunina, O. L. *J. Mol. Spectrosc.* **2000**, *202*, 229−248.
(44) Wang, X.; Andrews, L.; Gagliardi, L. *J. Phys. Chem. A* **2008**, *112*, 1754−61.
(45) Souter, P. F.; Kushto, G. P.; Andrews, L.; Neurock, M. *J. Phys. Chem. A* **1997**, *101*, 1287−1291.
(46) Souter, P. F.; Kushto, G. P.; Andrews, L.; Neurock, M. *J. Am. Chem. Soc.* **1997**, *119*, 1682−1687.
(47) Hunt, R. D.; Yustein, J. T.; Andrews, L. *J. Chem. Phys.* **1993**, *98*, 6070−6074.
(48) Li, J.; Bursten, B. E.; Liang, B.; Andrews, L. *Science* **2002**, *295*, 2242−2245.
(49) Barone, V. *J. Chem. Phys.* **2004**, *120*, 3059−3065.
(50) Barone, V. *J. Chem. Phys.* **2005**, *122*, 014108.
(51) Bloino, J.; Barone, V. *J. Chem. Phys.* **2012**, *136*, 124108.
(52) Bloino, J.; Biczysko, M.; Barone, V. *J. Chem. Theory Comput.* **2012**, *8*, 1015−1036.
(53) Pyykkö, P.; Atsumi, M. *Chem. - Eur. J.* **2009**, *15*, 12770−12779.
(54) Konings, R. J. M.; Benes, O. *J. Phys. Chem. Ref. Data* **2010**, *39*, 043102/1−043102/47.
(55) Konings, R. J. M.; Benes, O.; Kovacs, A.; Manara, D.; Sedmidubsky, D.; Gorokhov, L.; Iorish, V. S.; Yungman, V.; Shenyavskaya, E.; Osina, E. *J. Phys. Chem. Ref. Data* **2014**, *43*, 013101/1−013101/95.
(56) Cox, J. D.; Wagman, D. D.; Medvedev, V. A. In *CODATA Key Values for Thermodynamics*; Hemisphere: New York, 1989.
(57) Chase, M. W., Jr. *NIST-JANAF Thermochemical Tables*, 4th ed.; *J. Phys. Chem. Ref. Data, Monograph 9*, Supplement 1; American Institute of Physics: Woodbury, NY, 1998.
(58) Glendening, E. D.; Landis, C. R.; Weinhold, F. *J. Comput. Chem.* **2013**, *34*, 1429−1437.
(59) Weinhold, F. In *Encyclopedia of Computational Chemistry*; Schleyer, P. v. R., Ed.; John Wiley & Sons: Chichester, UK, 1998; Vol. 3, pp 1792−1811.
(60) Weinhold, F.; Landis, C. R. *Valency and Bonding: A Natural Bond Orbital Donor-Acceptor Perspective*; University Press: Cambridge, 2003.
(61) Reed, A. E.; Curtiss, L. A.; Weinhold, F. *Chem. Rev.* **1988**, *88*, 899−926.
(62) Matus, M. H.; Liu, S.-Y.; Dixon, D. A. *J. Phys. Chem. A* **2010**, *114*, 2644−2654.

DOI: 10.1021/acs.inorgchem.5b01383
Inorg. Chem. 2015, 54, 9761−9769